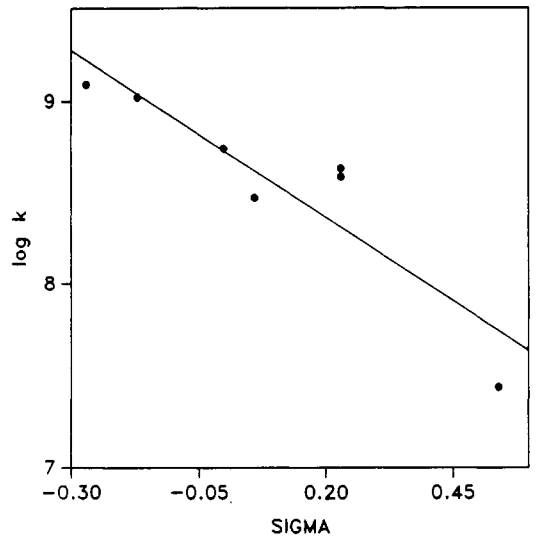

Figure 3. Plot of log k for the oxidation of 4-$XC_6H_4CH_2CrL(H_2O)^{2+}$ by $Ru(bpy)_3^{3+}$ versus the Hammett σ parameter for substituent X.

ratio (k^{py}/k^{Br} = 1.4), suggesting that for it the rates of reactions 3 and 7 are comparable.

Discussion

The reactivity of the $RCrL(H_2O)^{2+}$ complexes toward $Ru(bpy)_3^{3+}$ is very sensitive to the identity of the group R. In all, the rates vary by a factor of $\sim 10^8$ along the series. A similar trend is seen in the $*Cr(bpy)_3^{3+}$ rate constants, although here the reactivity is so much higher that the selectivity is less. The rates vary by a factor of only about 10^3 along the same series of R's.

We have thus made an effort to relate the measured rate constants to a fundamental parameter concerned with the electron-donating ability of the $RCrL(H_2O)^{2+}$ complexes. The ideal parameter would be values of $E°$ for the $RCrL(H_2O)^{3+/2+}$ couples. These, unfortunately, are currently unavailable. Thus we turned to the gas-phase ionization potentials of the alkyl radicals themselves, which have been measured by photoelectron spectroscopy.[50-53] For both series of reactions, Figure 2 depicts a plot of log k versus the ionization potential. Both series give a reasonable linear free energy correlation. This affirms that the nature of the reaction is indeed electron transfer.

In the series of $Ru(bpy)_3^{3+}$ reactions, rate constants were determined for a number of para-substituted benzyl groups (Table III). The more electron-donating substituents (e.g. CH_3O and CH_3) react more rapidly, whereas the smallest rate constant is that for CF_3, the substituent with the most positive σ value. A correlation according to the Hammett equation $\log k_x = \log k_H + \sigma\rho$ is shown in Figure 3. The reaction constant, given as the slope of this line, is ρ = −2.0.

The final question we would address concerns the rate at which the oxidized organochromium macrocycle undergoes homolysis in eq 3. A kinetic simulation was conducted for the overall scheme for R = C_2H_5. The value of k_3 was varied until the same rate was obtained for eq 1, regardless of whether $Co(NH_3)_5Br^{2+}$ or $Co(NH_3)_5py^{3+}$ was used as quencher. A value $k_3 < \sim 20\ s^{-1}$ was sufficient to account for the finding. If this same value of k_3 is assumed to apply to $1\text{-}C_3H_7CrL(H_2O)^{3+}$, it is possible through the same simulation to calculate the expected values of k with the two quenchers. (The value of k for the 1-propyl complex is smaller than for ethyl, and so the ratio between k^{py} and k^{Br} is not necessarily unity.) The simulation yields k^{py}/k^{Br} = 1.5, in reasonsable agreement with the experimental ratio of 1.4.

Conclusions. The family of $RCrL(H_2O)^{2+}$ complexes reacts with $Ru(bpy)_3^{3+}$ and $*Cr(bpy)_3^{3+}$ by electron transfer. The rate constants for electron transfer respond to a given alkyl or aralkyl group R such that k increases with the electron-donating ability of R, as measured by its ionization potential or Hammett σ constant. The resultant oxidized organometals $RCrL(H_2O)^{3+}$ undergo homolysis much more slowly than the pentaaqua analogues $(H_2O)_5CrR^{3+}$.

Acknowledgment. This research was supported by the U.S. Department of Energy, Office of Basic Energy Sciences, Chemical Sciences Division, under Contract W-7405-Eng-82.

(50) Houle, F. A.; Beauchamp, J. L. *J. Am. Chem. Soc.* **1978**, *100*, 3290.
(51) Taubert, R.; Lossing, F. P. *J. Am. Chem. Soc.* **1962**, *84*, 1523.
(52) Lossing, F. P.; DeSousa, J. B. *J. Am. Chem. Soc.* **1959**, *81*, 281.
(53) Houle, F. A.; Beauchamp, J. L. *J. Am. Chem. Soc.* **1979**, *101*, 4067.

Contribution from the Department of Chemistry,
Texas A&M University, College Station, Texas 77843

Further Studies on the Role of Neighboring Group Participation in CO Substitution Reactions of Group 6 Metal Carboxylates

Donald J. Darensbourg,* Jennifer A. Joyce, Christopher J. Bischoff, and Joseph H. Reibenspies

Received July 18, 1990

The reactions between $W(CO)_5O_2CR^-$ (R = $-C(CH_3)_3$, $-CH_2CN$, and $-CF_3$) and $P(OCH_3)_3$ result in cis CO replacement via a dissociative mechanism with concomitant formation of *cis*-$W(CO)_4[P(OCH_3)_3]O_2CR^-$. From the temperature dependence of the rate constants, activation parameters for the reactions where R = $-CH_2CN$ and $-C(CH_3)_3$ were determined to be ΔH^* = 25.3 ± 0.8 kcal·mol^{-1} and ΔS^* = 7.7 ± 2.5 eu and ΔH^* = 24.2 ● 1.5 kcal·mol^{-1} and ΔS^* = 9.7 ± 5.1 eu, respectively. These rate data, coupled with those previously reported for R = $-CH_3$ and −H, display a linear free energy relationship when plotted against Taft's polar substituent constant, σ^*. The reaction constant, ρ^*, was found to be −0.66, indicating the CO substitution reaction to be facilitated by electron-releasing substituents. This observation, taken together with the ability of the carboxylate ligand to chelate to the metal center, is interpreted as involvement of the distal oxygen atom of the monodentate carboxylate in cis CO substitution reactions. The X-ray structure of the cyanoacetate derivative, $[Et_4N][W(CO)_5O_2CCH_2CN]$, is also reported. The complex crystallizes in the triclinic centrosymmetric space group $P\bar{1}$ (No. 2) with a = 7.292 (2) Å, b = 11.552 (4) Å, c = 12.564 (4) Å, α = 76.03 (3)°, β = 73.65 (2) Å, γ = 86.48 (2) Å, V = 985.6 (5) Å^3, and Z = 2. Refinement converged at R = 2.36% and R_w = 3.23% for those 3380 reflections with $I > 2\sigma(I)$ and T = 193 K.

Introduction

As part of our continuing interest in the insertion chemistry of carbon dioxide into group 6 M–H and M–CH_3 bonds, we have investigated the kinetic parameters for CO dissociation in the resultant $M(CO)_5O_2CR^-$ (R = H, CH_3) derivatives.[1,2] Of particular concern is the role of metal unsaturation as a conse-

(1) Darensbourg, D. J.; Wiegreffe, H. P. *Inorg. Chem.* **1990**, *29*, 592.

0020-1669/91/1330-1137$02.50/0

quence of CO loss in the decarboxylation pathway of $M(CO)_5O_2CH^-$ species.[2-4] Thusfar, it has been clearly established that these carboxylate derivatives lose cis carbonyl ligands at a much faster rate than CO dissociation from the parent hexacarbonyls or their monosubstituted phosphine derivatives.[5,6] That is, in these anionic pentacarbonyl species, the carboxylate moiety is accurately defined as a *cis-labilizing* ligand.[7] On the contrary, the parent $RW(CO)_5^-$ (R = H or CH_3) derivatives do not possess labile cis carbonyl ligands.

By virtue of there being at least two functional groups in the carboxylate ligand, it is possible that part of the rate enhancement noted in the monodentate carboxylate derivatives involves the distal oxygen atom. The proximity of the distal oxygen atom of the monodentate-bound carboxylate ligand, coupled with its pronounced nucleophilic character,[8] can induce an intramolecular rate increase for CO dissociation. This might occur via the intermediacy of a bidentate carboxylate species (**1**), which subsequently undergoes facile ring opening because of strain resulting from the small bite angle of the carboxylate moiety (eq 1). The

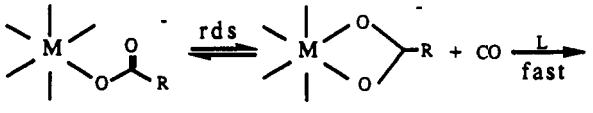

1

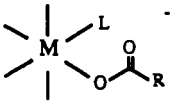

(1)

L = PR_3 or ^{13}CO

carboxylate's distal oxygen interaction depicted in **2** is most likely transitory to formation of species **1**. Alternatively, **2** may lead directly to substituted product without the intermediacy of chelate production.

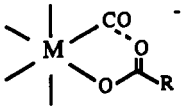

2

In an effort to determine the involvement of the distal oxygen atom of the mondentate carboxylate ligand in the CO labilization mechanism, we have studied the kinetic parameters for CO dissociation in $W(CO)_5O_2CR^-$, where R spans a range of electron-donating and electron-withdrawing substituents. If indeed the distal oxygen atom plays an intimate role in CO dissociation, there should be a correlation between the kinetic parameters for CO dissociation and the nucleophilicity of the uncoordinated oxygen atom.

Experimental Section

Materials. All manipulations were carried out either in an argon-filled drybox or on a double-manifold Schlenk vacuum line. Solvents were dried and degassed prior to use by distillation from sodium benzophenone ketyl under a nitrogen atmosphere. Tetrahydrofuran (THF) was purchased from J. T. Baker Chemical Co. Cyanoacetic acid, trimethylacetic acid sodium salt hydrate, [PPN][Cl] (PPN = bis(triphenylphosphine)-nitrogen(1+) cation), tetraethylammonium hydroxide (25% in methanol), and trimethyl phosphite were purchased from Aldrich Chemical Co. The phosphite was purified by distillation from sodium benzophenone ketyl under nitrogen prior to use. Trifluoroacetic acid was purchased from Sigma Chemical Co. Tungsten hexacarbonyl was purchased from Strem Chemicals, Inc. Carbon monoxide was obtained from Matheson Gas Products, Inc., and ^{13}CO (99% enriched) was purchased from Isotec, Inc. Experiments utilizing photolysis were performed with a mercury arc 450-W UV immersion lamp purchased from Ace Glass Co. Infrared spectra were recorded either on an IBM FTIR/32 or an IBM FTIR/85 spectrometer using a 0.1-mm NaCl solution cell. NMR spectra were taken on a Varian XL-200 superconducting high-resolution spectrometer with an internal deuterium lock in 5-mm tubes.

Synthesis of $[Et_4N][O_2CCH_2CN]$. To a solution of HO_2CCH_2CN (1.96 g, 2.30 mmol in 30 mL of methanol), Et_4NOH (14 mL, 0.0238 mol) was added via syringe. The solution was stirred at 40 °C for 1 h and the solvent removed under reduced pressure. The solid was dried at 60 °C in a vacuum drying oven and recrystallized from a mixture of acetonitrile and diethyl ether.

Synthesis of $[Et_4N][W(CO)_5O_2CCH_2CN]$. A solution of $[EtN_4][O_2CCH_2CN]$ (0.309 g, 1.44 mmol) and $W(CO)_6$ (0.405 g, 1.15 mmol) in 20 mL of dimethoxyethane (DME) was refluxed for 10 min. Hexane was added to the orange solution until solid precipitated. The solid was washed twice with hexane: IR ν(CO) 2061 (w), 1912 (s), 1858 (m) cm^{-1}. An X-ray-quality crystal was obtained by low-temperature recrystallization from a mixture of DME and hexane.

Synthesis of $[PPN][W(CO)_5O_2CCH_2CN]$. A solution of $W(CO)_6$ (0.877 g, 2.49 mmol in 60 mL of THF) was placed in a water-jacketed photolysis vessel and a vigorous stream of nitrogen bubbled through the solution. After 40–50 min of photolysis, an orange solution formed. IR indicated the major component to be of C_{4v} symmetry with a small amount of unreacted $W(CO)_6$; the species of C_{4v} symmetry was identified as $W(CO)_5THF$. The solution containing the THF adduct was added via cannula to a solution of $[PPN][O_2CCH_2CN]$[9] (1.02 g, 1.64 mmol in 60 mL of THF). The solution was stirred at 45 °C for 4 h. The orange solution was filtered and the solvent evaporated under reduced pressure. The product was recrystallized from THF and hexane to afford a yellow powder: 82% yield; IR ν(CO) 2062 (w), 1912 (s), 1849 (m) cm^{-1}; ^{13}C NMR (acetone-d_6) 201.1 (s), 205.5 ppm (s).

Synthesis of $[PPN][W(CO)_5O_2CC(CH_3)_3]$. The method of preparation was analogous to the above synthesis of $[PPN][W(CO)_5O_2CCH_2CN]$ using $W(CO)_6$ (0.859 g, 2.44 mmol) and $[PPN][O_2CC(CH_3)_3]$ (1.03 g, 1.61 mmol). An infrared spectrum of the bright orange solution that formed after stirring at room temperature for 1.5 h indicated a mixture of desired product and $[PPN][W(CO)_4(\eta^2\text{-}O_2CC(CH_3)_3)]$. Addition of CO gas resulted in a yellow solution in less than 5 min. Hexane was added, causing a solid to precipitate. The yellow solid was recrystallized from THF and hexane: 84% yield; IR ν(CO) 2058 (w), 1906 (s), 1841 (m) cm^{-1}; ^{13}C NMR, highly enriched in ^{13}CO (acetone-d_6), 202.0 (d), 206.5 ppm (p).

Synthesis of $[PPN][W(CO)_5O_2CCF_3]$. The method was similar to those described above using $[PPN][O_2CCF_3]$[9] (0.785 g, 1.21 mmol) and $W(CO)_6$ (0.639 g, 1.86 mmol). The reaction mixture was stirred at room temperature for 0.75 h. The solvent was removed under reduced pressure. The crude product was recrystallized from THF and hexane to afford a pale green solid: 81% yield; IR ν(CO) 2066 (w), 1916 (s), 1857 (m) cm^{-1}; ^{13}C NMR, enriched in ^{13}CO (acetone-d_6), 200.9 ppm (s).

Synthesis of $[PPN][W(CO)_4(\eta^2\text{-}O_2CC(CH_3)_3)]$. Two methods were used. In the first, a THF solution of $[PPN][W(CO)_5O_2CC(CH_3)_3]$ was heated at 50 °C for 1–2 h with a vigorous stream of nitrogen bubbling through the yellow solution. A bright orange solution was indicative of the chelated form. In the second method, a THF solution of $[PPN][W(CO)_5O_2CC(CH_3)_3]$ was placed in a water-jacketed photolysis vessel, and a vigorous stream of nitrogen was bubbled through the yellow solution. After 35–40 min of photolysis, a bright orange solution formed. For both methods of preparation, the IR spectrum of the orange solution indicated the major component to be of C_{2v} symmetry with contamination from the starting material. Addition of hexane to the solution resulted in formation of an orange oil that decomposed to starting material in 1–2 days at −20 °C. Attempts to isolate X-ray-quality crystals have thus far been unsuccessful: IR ν(CO) 1999 (w), 1859 (s), 1842 (m), 1808 (m) cm^{-1}.

Kinetic Measurements. The kinetics of carbonyl ligand substitution in $[PPN][W(CO)_5O_2CR]$ (R = $-CH_2CN$, $-C(CH_3)_3$, or $-CF_3$) by $P(OCH_3)_3$ were monitored by IR spectroscopy. Solution temperatures were controlled by a thermostated water bath with a precision of ±0.1 °C. To a solution of $[PPN][W(CO)_5O_2CR]$ (≈0.080 g) in THF (6.0 mL), $P(OCH_3)_3$ was added via syringe. Pseudo-first-order conditions were employed by using a large excess (>20 fold) of phosphite relative to metal complex. Small aliquots (≈0.2 mL) of solution were withdrawn

(2) Darensbourg, D. J.; Rokicki, A.; Darensbourg, M. Y. *J. Am. Chem. Soc.* **1981**, *103*, 3223.
(3) Darensbourg, D. J.; Wiegreffe, H. P.; Wiegreffe, P. W. *J. Am. Chem. Soc.* **1990**, *112*, 9252.
(4) Bo, C.; Dedieu, A. *Inorg. Chem.* **1989**, *28*, 304.
(5) Darensbourg, D. J. *Adv. Organomet. Chem.* **1982**, *21*, 113 and references therein.
(6) For example, the selective loss of cis CO ligands in the $[W(CO)_5O_2CCH_3]^-$ anion was definitively established by ^{13}C NMR analysis: Cotton, F. A.; Darensbourg, D. J.; Kolthammer, B. W. S.; Kudaroski, R. *Inorg. Chem.* **1982**, *21*, 1656.
(7) (a) Brown, T. L; Atwood, J. D. *J. Am. Chem. Soc.* **1976**, *98*, 3160. (b) Lichtenberger, D. L.; Brown, T. L. *J. Am. Chem. Soc.* **1978**, *100*, 366.
(8) Darensbourg, D. J.; Pala, M. *J. Am. Chem. Soc.* **1985**, *107*, 5687.
(9) Martiusen, A.; Songstad, J. *Acta. Chem. Scand., Ser. A* **1977**, *A31*, 645.

Table I. Crystallographic Data and Data Collection Parameters

formula	$C_{16}H_{22}N_2O_7W$
fw	538.2
space group	$P\bar{1}$, triclinic
a, Å	7.292 (2)
b, Å	11.552 (4)
c, Å	12.564 (4)
α, deg	76.03 (3)
β, deg	73.65 (2)
γ, deg	86.48 (2)
V, Å^3	985.6 (5)
Z	2
density (calc), g/cm^3	1.814
crystal size, mm	0.18 × 0.34 × 0.39
μ(Mo Kα), mm^{-1}	6.022
radiation	Mo Kα (λ = 0.710 73 Å)
scan type	θ–2θ
scan range	1.20° + Kα separation
2θ range, deg	4.0–50.0
no. of unique reflecns	3491 (R_{int} = 2.39%)
no. of obsd reflecns	3380 ($F > 4.0\sigma(F)$)
data param ratio	14.4:1
R, %	2.36
R_w, %	3.23
goodness of fit	2.37

periodically and examined by IR spectroscopy. The formation of *cis*-$[W(CO)_4[P(OCH_3)_3]O_2CR]^-$ was followed by measuring the appearance of the ν(CO) band at 2010 cm^{-1} for R = $-CH_2CN$ and at 2003 cm^{-1} for R = $-C(CH_3)_3$ as a function of time. A base-line correction was made on each spectrum by subtracting the absorbance in a region free of any absorbance peaks. These values were arbitrarily chosen as 2046 and 2048 cm^{-1}, respectively. Activation parameters were calculated by the method of Christian and Tucker.[10,11] Rate constants were determined by plotting ln $(A_i - A_t)$ versus time, where A_i is the IR absorbance at infinite time and A_t is the absorbance at a given time, t.

The kinetics of carbonyl ligand substitution in $[PPN][W(CO)_5O_2CCF_3]$ by $P(OCH_3)_3$ were similarly monitored. However, calculation of the rate constant was more complex due to formation of multiple products. The formation of *cis*-$[W(CO)_4[P(OCH_3)_3]O_2CCF_3]^-$ was determined by following the disappearance of the strong band of the starting material at 1915 cm^{-1} and the appearance of the band corresponding to $W(CO)_5P(OCH_3)_3$ at 1944 cm^{-1} as a function of time. A base-line correction was made on each spectrum by subtracting the absorbance at 2050 cm^{-1}. A rate constant for the loss of starting material was measured by plotting ln A at 1915 cm^{-1} as a function of time, after a correction was made for overlapping absorptions. The rate constant for the loss of $O_2CCF_3^-$ with concomitant formation of $W(CO)_5P(OCH_3)_3$ was measured by plotting ln $(A_i - A_t)$ at 1944 cm^{-1} as a function of time. The rate constant for formation of $[PPN][W(CO)_4[P(OCH_3)_3]O_2CCF_3]$ at 40 °C was taken to be the difference between these two values.

X-ray Structural Determination of $[Et_4N][W(CO)_5O_2CCH_2CN]$. A bright yellow parallelepiped (0.18 mm × 0.34 mm × 0.39 mm) was mounted on a glass fiber with vacuum grease at room temperature and cooled to 193 K in a N_2 cold stream. Preliminary examination and data collection was performed on a Nicolet R3m/V X-ray diffractometer (oriented graphite monochromator; Mo Kα λ = 0.710 73 Å radiation). Cell parameters were calculated from the least-squares fitting of the setting angles for 25 reflections. ω scans for several intense reflections indicated acceptable crystal quality. Data was collected for 4.0° ≤ 2θ ≤ 50.0° at 193 K. The scan range for the data collection was 1.20° plus Kα separation, with a variable scan rate of 1.50–15.00° min^{-1}. Background measurement by stationary crystal and stationary counter technique was done at the beginning and end of each scan for half of the total scan time. Lorentz and polarization corrections were applied to 3665 reflections. A semiempirical absorption correction was applied (T_{max} = 0.984, T_{min} = 0.669). Reflection intensities were profiled employing a learnt profile technique.[12] A total of 3380 unique observed reflections (R_{int} = 0.02) were used in further calculations. The structure was solved by direct methods (SHELXLS, SHELXTL-PLUS program package.[13] Full-matrix least-squares anisotropic refinement for all non-hydrogen atoms yielded R = 0.023, R_w = 0.032, and S = 2.37 at convergence. Hydrogen atoms were placed in idealized positions with isotropic thermal parameters fixed at 0.08. Neutral atom scattering factors were taken from ref 14. Crystal data and experimental conditions are provided in Table I.

Table II. K_{obs} as a Function of Temperature for the Reaction of $[PPN][W(CO)_5O_2CCH_2CN]$ with a 20-Fold Excess of $P(OCH_3)_3$[a]

temp, °C	10^3k_{obs}, s^{-1}	temp, °C	10^3k_{obs}, s^{-1}
31.8	0.238	45.0	1.55
36.0	0.427	50.0	2.54
40.0	0.744		

[a] Reactions were carried out in THF solution.

Table III. K_{obs} as a Function of Temperature for the Reaction of $[PPN][W(CO)_5O_2CC(CH_3)_3]$ with a 20-Fold Excess of $P(OCH_3)_3$[a]

temp, °C	10^3k_{obs}, s^{-1}	temp, °C	10^3k_{obs}, s^{-1}
23.0	1.02	28.0	2.25
24.5	1.31	30.0	3.02
26.0	1.75	32.0	3.46

[a] Reactions were carried out in THF solution.

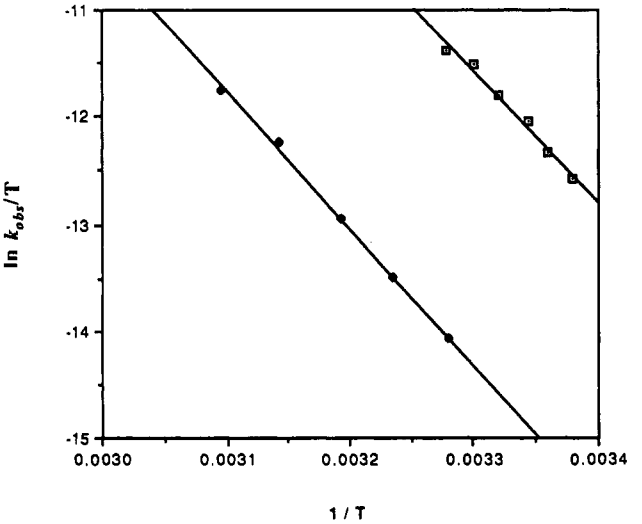

Figure 1. Eyring plots for the ligand substitution reactions of $[PPN][W(CO)_5L]$ with $P(OCH_3)_3$: (□) L = $-O_2CC(CH_3)_3$; (●) L = $-O_2CCH_2CN$.

Results

Carbon Monoxide Substitution in $[PPN][W(CO)_5O_2CR]$. The kinetic parameters for carbon monoxide ligand substitution reactions involving $[W(CO)_5O_2CR]^-$ (R = $-C(CH_3)_3$, $-CH_2CN$, and $-CF_3$) and trimethylphosphite (eq 2) have been determined

$$W(CO)_5O_2CR^- + P(OCH_3)_3 \rightleftharpoons cis\text{-}W(CO)_4[P(OCH_3)_3]O_2CR^- + CO \quad (2)$$

$$k_{obs} = \frac{k_1k_2[PR_3] + k_{-1}k_{-2}[CO]}{k_{-1}[CO] + k_2[PR_3]} \quad (3)$$

in THF solvent. The reactions were monitored by infrared spectroscopy in the ν(CO) region and were carried out by employing a 20-fold excess of $P(OCH_3)_3$, where the equilibrium process is shifted sufficiently to the right. In this instance, where $[P(OCH_3)_3] \gg [CO]$, the rate law expression (eq 3) reduces to $k_{obs} = k_1$ (vide infra).

The observed rate constants measured as a function of temperature for R = $-CH_2CN$ and $-C(CH_3)_3$ are listed in Tables II and III, respectively. Eyring plots of the data contained in Tables II and III (Figure 1) provide activation parameters of ΔH^* = 25.3 ± 0.8 kcal·mol^{-1} and ΔS^* = 7.7 ± 2.5 eu for R = $-CH_2CN$

(10) Christian, S. D.; Tucker, E. E. *Am. Lab (Fairfield, Conn.)* **1982**, *14* (8), 36.
(11) Christian, S. D.; Tucker, E. E. *Am. Lab (Fairfield, Conn.)* **1982**, *14* (9), 31.
(12) Diamond, R. *Acta. Crystallogr.* **1969**, *A25*, 43.
(13) Sheldrick, G. M. *SHELXTL-PLUS*, revision 3.4; Nicolet Instrument Corporation: Madison, WI, 1988.
(14) Cromer, D. T.; Waber, J. T. *International Tables for X-ray Crystallography*; Kynoch Press: Birmingham, England, 1974; Vol. IV, pp 55, 99.

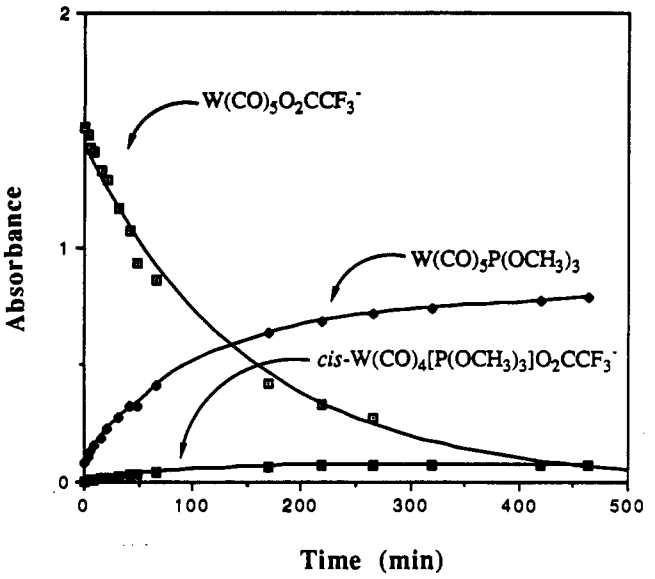

Figure 2. Disappearance and appearance of reactant and products in the reaction of $W(CO)_5O_2CCF_3^-$ with $P(OCH_3)_3$. The extinction coefficients of the ν(CO) IR bands monitored vary greatly.

and $\Delta H^* = 24.2 \pm 1.5$ kcal·mol^{-1} and $\Delta S^* = 9.7 \pm 5.1$ eu for R = $-C(CH_3)_3$.

Kinetic measurements of the rate of CO loss in the $W(CO)_5O_2CCF_3^-$ derivative were hampered by the concurrent displacement of the trifluoroacetate ligand by $P(OCH_3)_3$. That is, the sequence of reactions depicted in eq 4 were observed. Plots

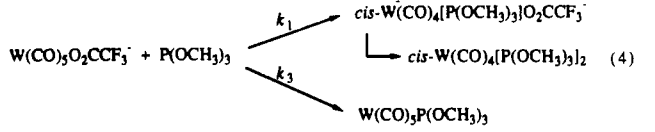

of the absorbance of the various species as a function of time are shown in Figure 2. The rate constants for dissociative loss of CO (k_1) and $O_2CCF_3^-$ (k_3) were measured at 40.0 °C and found to be comparable, with values of 1.23×10^{-4} and 1.30×10^{-4} s^{-1}, respectively. The product distribution of reaction 4 did not change significantly upon changing the temperature by 10 deg, thus indicating similar ΔH^* values for loss of both the carboxylate and the cis carbonyl ligands. This is to be contrasted with the situation noted for the other, less electron withdrawing, carboxylate ligands investigated, where CO loss is less energetic than carboxylate loss.

^{13}C NMR Experiments. The ^{13}C NMR spectrum of $[PPN][W(CO)_5O_2CCH_2CN]$, partially enriched with ^{13}CO, in acetone-d_6 indicated that the cis and trans carbonyl resonances occur at 201.1 and 206.0 ppm downfield from TMS, respectively. Because of the low level of ^{13}CO enrichment, both signals appeared as singlets. The cis W–C coupling constant was found to be 131.4 Hz.

The ^{13}C NMR spectrum of highly ^{13}CO enriched $[PPN][W(CO)_5O_2C(CH_3)_3]$ in acetone-d_6 indicated cis and trans carbonyl resonances at 202.0 and 206.4 ppm downfield from TMS, respectively. The cis carbonyl signal was split into a doublet, and the trans carbonyl signal was split into a pentet, with J_{C-C} being 2.4 Hz. The W–C coupling constant was determined to be 130.6 Hz for the cis carbonyl. Similarly, the ^{13}C NMR spectrum of ^{13}CO-enriched $[PPN][W(CO)_5O_2CCF_3]$ in acetone-d_6 exhibited signals for the cis carbonyls at 200.9 ppm; the trans carbonyl did not appear, and it is presumed that its signal is buried under the acetone peak at 206.1 ppm. The W–C coupling constant was determined to be 131.6 Hz.

Formation of Chelating Derivatives. The $[PPN][W(CO)_4(\eta^2\text{-}O_2CC(CH_3)_3]$ derivative was readily formed by thermolysis or photolysis. That is, heating a solution of $[PPN][W(CO)_5O_2CC(CH_3)_3]$ at 50 °C in THF under a vigorous stream of nitrogen resulted in nearly complete conversion to the chelated form of the complex, as indicated by infrared spectroscopy (see Figure 3). It is necessary to actively bubble nitrogen through the solution during the preparation of the chelated complex because of its rapid, thermal reaction with CO to re-form the monodentate complex. The infrared spectrum of the $[PPN][W(CO)_4(\eta^2\text{-}O_2CC(CH_3)_3)]$ product in THF exhibited ν(CO) stretching frequencies at 1999 (w), 1859 (s), 1842 (m), and 1808 (m) cm^{-1}. This pattern is consistent with a $W(CO)_4$ moiety of C_{2v} symmetry. The bonding nature of the carboxylate ligand can be surmised from the difference in the antisymmetric and symmetric stretching modes of the COO^- segment of the ligand.[15] In a THF solution of $[PPN][W(CO)_5O_2CC(CH_3)_3]$, $\nu_a(COO^-)$ and $\nu_s(COO^-)$ are observed at 1610 and 1390 cm^{-1}, respectively. The difference in these vibrations $[\nu_a(COO^-) - \nu_s(COO^-)]$ is 220 cm^{-1}, which is as expected for a monodentate carboxylate. Upon formation of the chelate species, $\nu_a(COO^-)$ and $\nu_s(COO^-)$ are seen at 1523 and 1438 cm^{-1}, or their difference is 85 cm^{-1}, which is consistent with a chelating carboxylate ligand. The assignments of $\nu_a(COO^-)$ and $\nu_s(COO^-)$ were partially based upon analogy with $[PPN][W(CO)_5O_2CCH_3]$.[1]

Conversely, $[PPN][W(CO)_4(\eta^2\text{-}O_2CCH_2CN)]$ was not detected in the thermal reaction. However, prolonged photolysis (3.5 h) of $[PPN][W(CO)_5O_2CCH_2CN]$ resulted in trace quantities of the chelated derivative, as observed by infrared spectroscopy.

Solid-State Structure of $[Et_4N][W(CO)_5O_2CCH_2CN]$. The molecular structure of $[Et_4N][W(CO)_5O_2CCH_2CN]$ was defined by single-crystal X-ray diffraction. Bright yellow crystals suitable for X-ray analysis were isolated from THF/hexane. The crystal

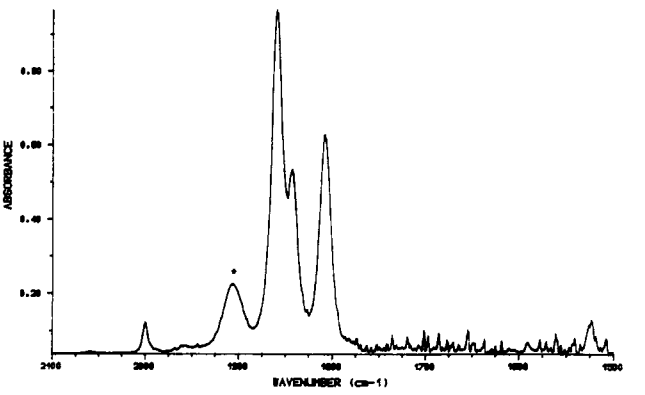

Figure 3. Infrared spectrum of $[PPN][W(CO)_4(\eta^2\text{-}O_2CC(CH_3)_3)]$. The asterisk marks unreacted $[PPN][W(CO)_5O_2CC(CH_3)_3]$.

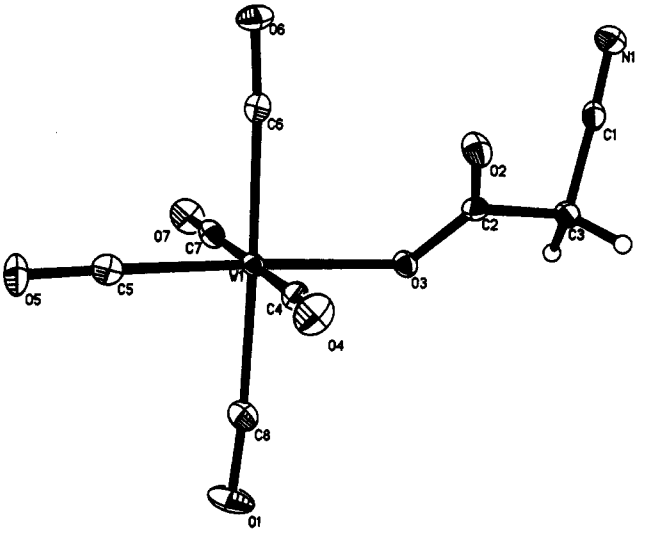

Figure 4. Thermal ellipsoid plot of $[W(CO)_5O_2CCH_2CN]^-$.

(15) Nakamoto, K. *Infrared and Raman Spectra of Inorganic and Coordination Compounds*, 4th ed.; Wiley: New York, 1986; p 231.
(16) Cotton, F. A.; Darensbourg, D. J.; Kolthammer, B. W. S. *J. Am. Chem. Soc.* **1981**, *103*, 398.

Table IV. Atomic Coordinates ($\times 10^4$) and Equivalent Isotropic Displacement Parameters ($Å^2 \times 10^3$) for $[Et_4N][W(CO)_5O_2CCH_2CN]$

	x	y	z	U(eq)[a]
W(1)	5659 (1)	3165 (1)	8119 (1)	22 (1)
O(3)	6077 (4)	4381 (3)	6405 (3)	29 (1)
O(2)	8713 (4)	5273 (3)	6391 (3)	40 (1)
N(100)	8686 (5)	1853 (3)	2579 (3)	23 (1)
O(6)	7159 (5)	5057 (3)	9173 (3)	42 (1)
C(7)	2934 (7)	3806 (4)	8518 (4)	34 (2)
O(4)	9880 (5)	2115 (3)	7699 (3)	46 (1)
C(8)	4787 (7)	1850 (4)	7548 (4)	35 (2)
O(7)	1398 (5)	4162 (3)	8792 (3)	49 (2)
C(6)	6634 (6)	4410 (4)	8761 (4)	31 (1)
O(5)	4758 (5)	1412 (3)	10522 (3)	46 (1)
C(5)	5094 (6)	2081 (4)	9626 (4)	31 (2)
O(1)	4331 (6)	1042 (3)	7299 (4)	60 (2)
C(4)	8373 (6)	2522 (4)	7796 (4)	30 (2)
C(3)	7392 (6)	5969 (4)	4826 (4)	30 (1)
C(2)	7419 (6)	5142 (4)	5982 (4)	27 (1)
C(107)	9112 (6)	591 (4)	3165 (4)	33 (2)
N(1)	7487 (7)	8166 (3)	4983 (4)	47 (2)
C(106)	9121 (6)	2761 (4)	3165 (4)	32 (2)
C(105)	6593 (6)	1854 (4)	2620 (4)	31 (1)
C(104)	9839 (8)	1298 (5)	634 (4)	47 (2)
C(103)	7947 (7)	2626 (5)	4386 (4)	44 (2)
C(1)	7463 (6)	7218 (4)	4886 (3)	32 (2)
C(102)	9932 (7)	2186 (4)	1350 (4)	35 (2)
C(101)	11196 (7)	354 (4)	3162 (4)	41 (2)
C(100)	5820 (7)	3059 (4)	2151 (4)	41 (2)

[a] Equivalent isotropic U defined as one-third of the trace of the orthogonalized U_{ij} tensor.

Table V. Bond Lengths (Å) for $[Et_4N][W(CO)_5O_2CCH_2CN]$

W(1)–O(3)	2.220 (3)	W(1)–C(7)	2.045 (5)
W(1)–C(8)	2.033 (6)	W(1)–C(6)	2.056 (5)
W(1)–C(5)	1.950 (4)	W(1)–C(4)	2.036 (5)
O(3)–C(2)	1.264 (5)	O(2)–C(2)	1.227 (6)
N(100)–C(107)	1.523 (5)	N(100)–C(106)	1.513 (7)
N(100)–C(105)	1.512 (6)	N(100)–C(102)	1.524 (5)
O(6)–C(6)	1.142 (7)	C(7)–O(7)	1.156 (6)
O(4)–C(4)	1.155 (6)	C(8)–O(1)	1.148 (7)
O(5)–C(5)	1.172 (5)	C(3)–C(2)	1.539 (6)
C(3)–C(1)	1.468 (7)	C(107)–C(101)	1.526 (7)
N(1)–C(1)	1.132 (7)	C(106)–C(103)	1.508 (6)
C(105)–C(100)	1.516 (6)	C(104)–C(102)	1.534 (8)

Table VI. Bond Angles (deg) for $[Et_4N][W(CO)_5O_2CCH_2CN]$

O(3)–W(1)–C(7)	87.1 (1)	O(3)–W(1)–C(8)	89.9 (2)
C(7)–W(1)–C(8)	90.9 (2)	O(3)–W(1)–C(6)	93.1 (1)
C(7)–W(1)–C(6)	91.7 (2)	C(8)–W(1)–C(6)	176.1 (2)
O(3)–W(1)–C(5)	175.7 (2)	C(7)–W(1)–C(5)	89.4 (2)
C(8)–W(1)–C(5)	87.7 (2)	C(6)–W(1)–C(5)	89.5 (2)
O(3)–W(1)–C(4)	95.0 (1)	C(7)–W(1)–C(4)	177.5 (2)
C(8)–W(1)–C(4)	90.6 (2)	C(6)–W(1)–C(4)	86.8 (2)
C(5)–W(1)–C(4)	88.6 (2)	W(1)–O(3)–C(2)	122.4 (3)
C(107)–N(100)–C(106)	111.3 (4)	C(107)–N(100)–C(105)	105.9 (3)
C(106)–N(100)–C(105)	111.6 (3)	C(107)–N(100)–C(102)	110.8 (3)
C(106)–N(100)–C(102)	106.4 (3)	C(105)–N(100)–C(102)	110.9 (4)
W(1)–C(7)–O(7)	177.0 (5)	W(1)–C(8)–O(1)	174.4 (4)
W(1)–C(6)–O(6)	176.2 (4)	W(1)–C(5)–O(5)	178.7 (5)
W(1)–C(4)–O(4)	174.8 (4)	C(2)–C(3)–C(1)	109.7 (4)
O(3)–C(2)–O(2)	126.9 (4)	O(3)–C(2)–C(3)	115.0 (4)
O(2)–C(2)–C(3)	118.0 (4)	N(100)–C(107)–C(101)	115.4 (3)
N(100)–C(106)–C(103)	114.8 (4)	N(100)–C(105)–C(100)	114.8 (3)
C(3)–C(1)–N(1)	177.0 (4)	N(100)–C(102)–C(104)	114.6 (4)

was mounted in open air at room temperature and immediately cooled to 193 K. Final atomic coordinates for all non-hydrogen atoms are given in Table IV. One complete cation and one complete anion were found in the unique volume of the unit cell. A view of the anion is shown in Figure 4. Bond lengths and bond angles for the complex are listed in Tables V and VI.

The complex exists as a slightly distorted octahedron. The average W–C bond distance for the cis carbonyl ligands is 2.043 (5) Å, whereas the W–C bond distance for the trans carbonyl ligand is shorter at 1.950 (4) Å. The average C(trans)–W–C(cis) bond angle is 88.8 (4)°. The carboxylate ligand is positioned 2.220 (3) Å away from the tungsten atom diagonally in the plane of the cis carbonyl ligands so that the distal oxygen atom lies directly between two carbonyl carbon atoms. The nitrogen atom is sufficiently removed from the metal center and positioned so as to be noninteractive with the metal or the carbonyl ligands. Table VII compares selected bond distances and angles for tungsten pentacarbonyl carboxylate derivatives that have thusfar been characterized by X-ray crystallography.[6,8]

Table VII. Comparative Bond Distances (Å) and Angles (deg) in $W(CO)_5O_2CR^-$ Derivatives

R	W–O	W–CO_{cis} (av)	W–CO_{trans}	∠O–W–C_{cis} (av)
–H[a]	2.216 (15)	2.037 (13)	1.911 (15)	91.8
$-CH_3$[b]	2.207 (4)	2.038 (18)	1.951 (6)	91.4
$-CH_2CN$	2.220 (3)	2.043 (5)	1.950 (4)	92.2

[a] Taken from ref 8. [b] Taken from ref 6.

Table VIII. Taft Data for the Ligand Exchange Reactions of $[PPN][W(CO)_5O_2CR]$ with $P(OCH_3)_3$[a]

R	σ*	$10^3 k_{obs}$(40 °C), s^{-1}
$-C(CH_3)_3$	−0.30	10.9
$-CH_3$	0.00	5.55
–H	0.49	2.86
$-CH_2CN$	1.30	0.744
$-CF_3$	2.61	0.123

[a] Reactions were seen in THF solution.

Scheme I

$$W(CO)_5O_2CR^- \underset{k_{-1}}{\overset{k_1}{\rightleftharpoons}} \{M(CO)_4O_2CR^-\} + CO$$

3

$$k_{-2} \Big\| k_2\ [PR_3]$$

cis-$M(CO)_4(PR_3)O_2CR^-$

Discussion

The cis-labilizing ability of ligands capable of π-donation to the metal center in d^6 metal pentacarbonyls, $M(CO)_5X^{n-}$ (n = 0, 1), is well established. In general, systematic studies quantifying the kinetic parameters for cis CO dissociation as a function of substituents (electron donating and withdrawing) on the unique ligand (X) are noticeably absent. We have begun extensive investigations to rectify this deficiency. Although our current focus centers on carboxylate ligands because of their relationship to CO_2 insertion reactions, we hope to extend these studies to a variety of groups, in particular alkoxides and aryloxides. The cis-labilizing ligand examined in this report, the carboxylate ligand, is complicated in that two effects can operate simultaneously. Specifically, a rate phenomenon originating in the M–O bond may be operative of the type discussed by Brown et al.,[7] i.e., due to the π-donicity of the X group and/or preferred geometry of the five-coordinate fragment. In addition, the carboxylate's distal oxygen atom can assist in the loss of a cis carbonyl ligand.

The CO substitution reaction involving carboxylate derivatives of tungsten pentacarbonyl with phosphorus donor ligands (Scheme I) follows the rate law defined in eq 3 for an equilibrium process. This is the case whether **3** represents the intermediacy of an unsaturated five-coordinate species or a saturated chelating carboxylate derivative. The rate constants for cis CO dissociation, k_1, determined as a function of the R substituent are listed in Table VIII and represented in Figure 5 as a Taft plot ($\log k_1 = \rho^*\sigma^*$), where σ^* is the polar substituent constant.[17] The reaction constant, ρ^*, was found to be −0.66, indicating the ligand substitution reaction to be facilitated by electron-releasing substituents. It

(17) Taft, R. W. *J. Am. Chem. Soc.* **1952**, *74*, 3120.

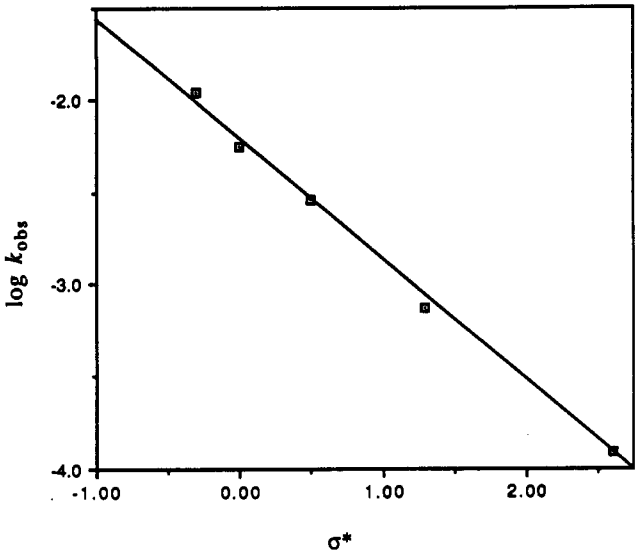

Figure 5. Taft plot for the reaction of [PPN][$W(CO)_5O_2CR$] with $P(OCH_3)_3$ at 40 °C for R = $-C(CH_3)_3$, $-CH_3$, $-H$, $-CH_2CN$, and $-CF_3$.

is noteworthy that the Taft plot encompasses a wide range of σ^* values, from −0.30 for R = $-C(CH_3)_3$ to +2.61 for R = $-CF_3$, with the corresponding rate constants extending over 2 orders of magnitude. The reaction constant is somewhat smaller than that of 1.62 noted for formic acid (RCOOH, $pK_a° = 4.66$ and log $K_a/K_a° = \rho^*\sigma^*$) and more closely resembles that found for insertion of a saturated carbon unit between the R substituent and the carboxylate function; i.e., RCH_2COOH has a ρ^* value of −0.67. Nevertheless, the effect is quite significant, clearly indicating that more electron-donating carboxylate ligands lead to more labile CO groups.

This observation alone does not allow us to distinguish between effects operative via the W–O bond directly and those originating from the distal oxygen interaction at a carbonyl ligand site. For example, a linear free energy relationship is noted between k_1 and k_{CO}, the CO stretching force constant[18] of the trans CO ligand in $W(CO)_5O_2CR^-$ derivatives. It is specifically this CO vibrational mode that should be most influenced by the nature of the W–O bond. There is however a strong correlation between the ability of the carboxylate to chelate and the rate of cis CO dissociation. That is, chelation of the carboxylate ligand is observed in instances where the distal oxygen is electron-rich, e.g., R = $-C(CH_3)_3$, $-CH_3$, and $-H$, and is not seen for electron-withdrawing substituents R = $-CH_2CN$ or $-CF_3$. The solid-state structures of members from each category, R = $-CH_3$ and $-H$ and R = $-CH_2CN$, are extremely similar, with average distal oxygen to cis CO ligands distances being identical. It is furthermore of interest to note that the nitrile group of the cyanoacetate ligand, upon rotation about the O(3)–C(2) bond, does not provide good orbital direction for interaction with the metal via the lone pair on nitrogen. However, donation of π-electron density via the $-C\equiv N$ linkage is possible. This is a point of importance in decarboxylation processes, where interaction of the substituent on the carboxylate ligand with the metal center is thought to be a prerequisite for carbon dioxide extrustion.[19,20]

Hence, we feel that these latter observations, coupled with the rapid reaction rates observed for these chelated species with CO or $P(OCH_3)_3$ (e.g., reaction 5) argue in favor of an involvement of the distal oxygen atom. This is reinforced by the results for

$$W(CO)_4(\eta^2\text{-}O_2CC(CH_3)_3)^- + P(OCH_3)_3 \rightarrow cis\text{-}W(CO)_4[P(OCH_3)_3]O_2CC(CH_3)_3^- \quad (5)$$

CO substitution processes involving the $Cr(CO)_5O_2CCH_3^-$ derivative,[2] where the effect is more pronounced. The smaller metal center enhances distal oxygen cis carbonyl ligand interactions, as indicated by the activation parameters for CO substitution. The small "bite" angle for the carboxylate ligand[21,22] of approximately 60° results in better orbital interactions with the chromium center than with the larger tungsten center.

Our future plan is to examine the magnitude of through bond substituent effect by investigating metal pentacarbonyl aryloxides ($-OC_6H_4X$), where there is no distal oxygen and where comparable changes in ν(CO) or k_{CO} to those observed here for $-O_2CR^-$ derivatives are noted. With regard to metal carboxylates, an interesting prediction that our observations allow us to make at this point is that CO loss from metal pentacarbonyl aryl carbonates ($-O_2COPh$), the products of CO_2 insertion into metal–OPh bonds,[23,24] will be slow ($-OPh$, $\sigma^* = +2.32$) and for the metal pentacarbonyl oxalates will be fast ($-CO_2^-$, $\sigma^* = -1.06$). Preliminary results support these expectations.[25] Furthermore, based on the value of σ^* for $-OH$ vs $-O^-$,[26] the bicarbonate product that results from the hydrolysis of $(CO)_5WO_2COPh^-$ would be expected to be deprotonated by base prior to ring closure (eq 6).[21,23] That

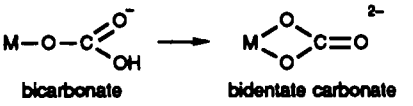

(6)

is, formation of $(CO)_5MCO_3^{2-}$ should be an intermediate step in eq 6. Bicarbonate and carbonate species analogous to these have been spectroscopically observed during the surface reactions of Cr_2O_3 with carbon monoxide.[27]

Acknowledgment. The financial support of this research by the National Science Foundation (Grant 88-17873) is greatly appreciated.

Supplementary Material Available: Tables of refined anisotropic thermal parameters, final fractional coordinates, and thermal parameters for hydrogen atoms (2 pages); a listing of observed and calculated structure factors (13 pages). Ordering information is given on any current masthead page.

(18) Cotton, F. A.; Kraihanzel, C. S. *J. Am. Chem. Soc.* **1962**, *84*, 4432.
(19) Deacon, G. B.; Faulks, S. J.; Pain, G. N. *Adv. Organomet. Chem.* **1986**, *25*, 237.
(20) Darensbourg, D. J.; Joyce, J. A. Unpublished observations.
(21) Darensbourg, D. J.; Sanchez, K. M.; Rheingold, A. L. *J. Am. Chem. Soc.* **1987**, *109*, 290.
(22) Recently we have completed an X-ray structural analysis of [PPN][$W(CO)_4(\eta^2\text{-}S_2CCH_3)$] where the S–W–S angle is 67.0°: Darensbourg, D. J.; Wiegreffe, H. P. *Organometallics*, in press.
(23) Darensbourg, D. J.; Sanchez, K. M.; Reibenspies, J. H.; Rheingold, A. L. *J. Am. Chem. Soc.* **1989**, *111*, 7094.
(24) Darensbourg, D. J.; Mueller, B. L.; Reibenspies, J. H.; Bischoff, C. J. *Inorg. Chem.* **1990**, *29*, 1789.
(25) The oxalate ligand reacts with $W(CO)_5THF$ to initially provide oxalate-bridged tungsten dimers that ultimately lead to the very stable chelated dimer, where oxygen atoms of adjacent carbon centers bind to each tungsten center. The resultant [PPN][$W_2(CO)_8C_2O_4$] complex has been characterized by X-ray crystallography: Joyce, J. A. Unpublished results.
(26) Taken from: *Lange's Handbook*, 12th ed.; Dean, J. A., Ed.; McGraw-Hill, New York, 1979.
(27) Lokhov, Yu. A.; Bredikhin, M. N. Cited in: Bruker report; Bruker Instruments, Inc., San Jose, CA, 1990; p 12.